Increased O-GlcNAcylation rapidly decreases $GABA_AR$ currents in hippocampus yet depresses neuronal output

Luke T. Stewart[1*], Kavitha Abiraman[1*], John C. Chatham[2], Lori L. McMahon[1#]

[1] Department of Cell, Developmental and Integrative Biology , University of Alabama at Birmingham, Birmingham, AL 35294

[2] Department of Pathology, University of Alabama at Birmingham, Birmingham, AL 35294

[#] corresponding author: mcmahon@uab.edu

* authors contributed equally

Abstract

O-GlcNAcylation, a post-translational modification involving O-linkage of β-N-acetylglucosamine to Ser/Thr residues on target proteins, is increasingly recognized as a critical regulator of brain function in health and disease. Enzymes that catalyze O-GlcNAcylation are found at both presynaptic and postsynaptic sites, and O-GlcNAcylated proteins localize to synaptosomes. Acute increase in O-GlcNAcylation induces long-term depression (LTD) of excitatory transmission at hippocampal CA3-CA1 synapses, and depresses hyperexcitable circuits in vitro and in vivo. Yet, no study has investigated how O-GlcNAcylation modulates the efficacy of inhibitory neurotransmission. Here we show an acute increase in O-GlcNAc dampens GABAergic currents onto principal cells in rodent hippocampus likely through a postsynaptic mechanism, and increases the excitation/inhibition balance. However, the overall effect of increased O-GlcNAc is reduced synaptically-driven spike probability via decreased intrinsic excitability and synaptic depression. Our results position O-GlcNAcylation as a novel regulator of the excitation/inhibition balance and neuronal output.

Introduction

Synaptic integration and spike initiation in neurons is controlled by synaptic inhibition, which strongly influences neuronal output and information processing (Farrant and Nusser, 2005). Importantly, the balance of excitation to inhibition (E/I) is crucial to the proper functioning of circuits, and E/I imbalances have been implicated in a number of neurodevelopmental disorders and neurodegenerative diseases including schizophrenia, autism spectrum disorders, and Alzheimer's disease (Fernandez et al., 2007; Gogolla et al., 2009; Kehrer et al., 2008; Roberson et al., 2011). Thus, understanding the mechanisms that modulate the strength of inhibitory transmission is fundamental to unraveling how neuronal circuits function in normal and disease states.

Fast inhibitory transmission in the central nervous system is mediated by $GABA_A$ receptors ($GABA_ARs$), which are pentameric ligand-gated ion channels. The strength of this inhibition can be rapidly up- or down-regulated by post-translational modifications including ubiquitination (Saliba et al., 2007), palmitoylation (Keller et al., 2004; Rathenberg et al., 2004), and phosphorylation (Nakamura et al., 2015) of $GABA_AR$ subunits and/or associated proteins, which can alter channel function, trafficking, or stability at the membrane. While there is a vast body of literature on these post-translational modifications, O-GlcNAcylation, involving the O-linkage of β-N-acetylglucosamine (O-GlcNAc) to Ser/Thr residues on target proteins, remains severely understudied, with no examination to date of the effect of protein O-GlcNAcylation on inhibitory synapse physiology.

Addition and removal of O-GlcNAc are catalyzed by the single pair of enzymes O-GlcNAc transferase (OGT) and O-GlcNAcase (OGA), and is essential as genetic deletion of OGT and OGA are lethal (Keembiyehetty et al., 2015; Shafi et al., 2000). O-GlcNAcylation is metabolically-regulated and highly dynamic; global changes reversibly occur within minutes, and are dictated by availability of UDP-GlcNAc, which is synthesized from glucose via the hexosamine biosynthetic pathway (HBP) (Yang and Qian, 2017). The brain contains the second highest level of O-GlcNAcylated proteins in the body (Kreppel et al., 1997), with the hippocampus expressing one of the highest levels of OGT/OGA (Liu et al., 2004b). Notably, the majority of O-GlcNAcylated proteins are found at the synapse (Trinidad et al., 2012). However, only a handful of studies have examined the functional impact of O-GlcNAcylation in the brain (Lagerlöf et al., 2017; Ruan et al., 2014; Stewart et al., 2017; Taylor et al., 2014; Yang et al., 2017).

Previous work from our lab has examined the role of protein O-GlcNAcylation at glutamatergic synapses in hippocampal area CA1, where O-GlcNAcylation of the AMPA receptor (AMPAR) GluA2 subunit initiates long-term synaptic depression, termed 'O-GlcNAc LTD' (Taylor et al., 2014). Recent work (Hwang and Rhim, 2019) showing that increased O-GlcNAc suppresses excitatory transmission at CA3-CA1 synapses through the removal of GluA2 containing AMPARs is consistent with our findings. Additionally, increased O-GlcNAcylation dampens picrotoxin-induced epileptiform activity in area CA1 and CA3, and reduces seizure activity in the pentylenetetrazole in vivo model of seizure activity in mice (Stewart et al., 2017). Deletion of OGT in αCaMKII expressing neurons in the adult rodent brain causes a reduction in excitatory synaptic input onto hypothalamic PVN neurons (Lagerlöf et al., 2016), while OGT knock-out (KO) specifically from hypothalamic AgRP neurons reduces excitability via its effect on voltage-gated potassium channels (Ruan et al., 2014). Conversely, no studies to date have examined the role of protein O-GlcNAcylation in inhibitory synaptic function. Because serine phosphorylation of $GABA_AR$ subunits regulates the efficacy of neuronal inhibition (McDonald and Moss, 1997; Vithlani et al., 2011), it is highly likely that serine O-GlcNAcylation will also control $GABA_AR$ function.

Here, we show that an acute increase in protein O-GlcNAcylation rapidly induces a long-lasting decrease in strength of GABAergic synaptic transmission in hippocampus that is likely through an effect on post-synaptic $GABA_A$Rs. This depression of inhibition produces a net increase in the excitation/inhibition ratio. However, despite the increase in E/I balance, the overall effect is a depression of neuronal output due to a simultaneous decrease in intrinsic excitability together with reduced synaptic drive at both excitatory and inhibitory synapses. Thus, global changes in O-GlcNAcylation induce complex changes in network activity by targeting excitatory and inhibitory synapses together with direct effects on intrinsic excitability.

Results

Acute increase in protein O-GlcNAcylation depresses GABAergic transmission onto CA1 pyramidal cells and dentate granule cells

To determine if protein O-GlcNAcylation modulates $GABA_A$R-mediated inhibitory neurotransmission, we used whole-cell voltage clamp to record spontaneous inhibitory post-synaptic currents (sIPSCs) from CA1 pyramidal cells while blocking glutamatergic transmission using DNQX (10 μM) and DL-AP5 (50 μM). Following a 5 min baseline, we bath applied the HBP substrate glucosamine (GlcN, 5mM) and the OGA inhibitor thiamet-G (TMG, 1μM) to acutely increase protein O-GlcNAc levels, as done previously (Stewart et al., 2017; Taylor et al., 2014) (Fig 1Ai).

We found a significant reduction in sIPSC amplitude (Fig 1Aii, cumulative probability distribution of amplitude, p<0.0001, KS D value = 0.217, Kolmogorov-Smirnov test; inset: p<0.0001, Wilcoxon matched-pairs signed rank test) and inter-event interval (Fig 1Aiii, cumulative probability distribution of inter-event interval, p<0.0001, KS D value = 0.084, Kolmogorov-Smirnov test; inset: p<0.0001, Wilcoxon matched-pairs signed rank test) in CA1 pyramidal cells. To ensure that the change in amplitude and inter-event interval was not a consequence of an increase in series resistance, which decreases the amplitude and slows the rise/decay of synaptic events, sIPSCs during baseline and 5 min after GlcN+TMG application were averaged and scaled; no difference in the time course was observed (data not shown). It is also important to note that we observed a shift in holding current following application of GlcN+TMG (baseline: -138.2±13.6 pA vs. GlcN+TMG: -106.4±11.5 pA, p=0.006, paired t-test), suggesting a possible effect on extrasynaptic $GABA_A$Rs, which will be investigated in future experiments.

In order to determine if this decrease in sIPSCs induced by GlcN+TMG is specific to CA1 pyramidal cells or if it occurs at inhibitory synapses on other cells, we recorded sIPSCs from dentate gyrus granule cells (GCs) before and after bath application of GlcN+TMG (Fig 1Bi). We observed the same effect, namely a decrease in sIPSC amplitude (Fig 1Bii, cumulative probability distribution of amplitude, p<0.0001, KS D value = 0.109, Kolmogorov-Smirnov test; inset: p<0.0001, Wilcoxon matched-pairs signed rank test) and increase in inter-event interval (Fig 1Biii, cumulative

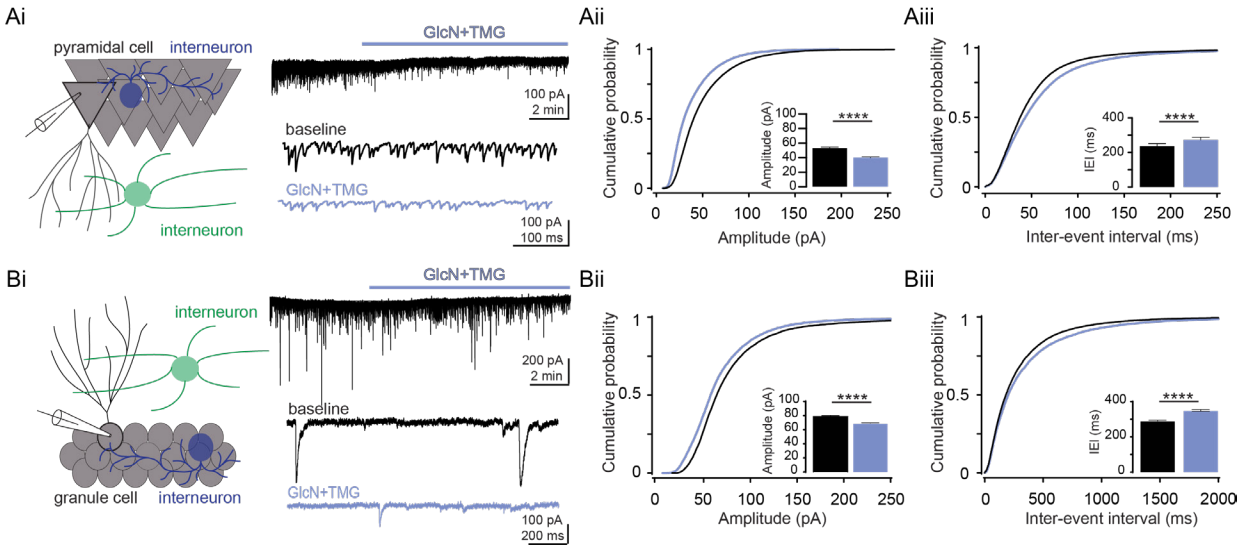

Figure 1: Acute increase in O-GlcNAcylation reduces spontaneous IPSCs in hippocampal principal cells
(Ai) (left) Schematic depicting recording set up in CA1. (right) representative sIPSC trace from CA1 pyramidal cell showing (top) GlcN+TMG wash on and (bottom) expanded time scale (control (black) and GlcN+TMG (blue)). (Aii) Cumulative probability distribution of sIPSC amplitude (p<0.0001, KS D value = 0.084, Kolmogorov-Smirnov test); inset: average (±SEM) sIPSC amplitude. Baseline: 43.1±0.5pA, GlcN+TMG: 31.4±0.4 pA (p<0.0001, Wilcoxon matched-pairs signed rank test, n=9 cells, 5 rats) (Aiii) Cumulative probability distribution of sIPSC IEI p<0.0001, KS D value = 0.084, Kolmogorov-Smirnov test; inset: average (± SEM) sIPSC inter-event interval (IEI). Baseline: 53.1±0.9 ms, GlcN+TMG: 62.4±1.2 ms (p<0.0001, Wilcoxon matched-pairs signed rank test, n=9 cells, 5 rats) (Bi) (left) Schematic depicting recording set up in dentate gyrus and (right) representative sIPSC trace from a granule cell showing (top) GlcN+TMG wash on and (bottom) expanded time scale. (Bii) Cumulative probability distribution of sIPSC amplitude (p<0.0001, KS D value = 0.11, Kolmogorov-Smirnov test); inset: average (± SEM) sIPSC amplitude. Baseline: 78.91±0.61pA, GlcN+TMG: 69.10±0.54 pA (p<0.0001, Wilcoxon matched-pairs signed rank test, n=11 cells, 7 rats). (Biii) Cumulative probability distribution of sIPSC IEI; inset: average (± SEM) sIPSC IEI (p<0.0001, KS D value = 0.055 ,Kolmogorov-Smirnov test). Baseline: 301.4±3.6 ms, GlcN+TMG: 349.5±4.7 ms (p<0.0001, Wilcoxon matched-pairs signed rank test, n=11 cells, 7 rats). ****p<0.0001.

probability distribution of inter-event interval, p<0.0001, KS D value = 0.055 , Kolmogorov-Smirnov test; inset: p<0.0001, Wilcoxon matched-pairs signed rank test), but no shift in holding current (p=0.768, paired t-test). These findings suggest that O-GlcNAc-mediated depression of GABAergic transmission is likely to be a general mechanism occurring at many inhibitory synapses in the brain.

The decrease in sIPSCs following increased O-GlcNAcylation could arise from a decrease in presynaptic GABA release, or from decreased postsynaptic $GABA_AR$ function. To distinguish between these possibilities, we recorded mIPSCs from both CA1 pyramidal cells and GCs in the presence of the voltage-gated sodium channel blocker TTX (1 μM) (Fig 2Ai and 2Bi). A change in mIPSC frequency typically reflects a change in presynaptic neurotransmitter release probability, while a change in mIPSC amplitude indicates a change in postsynaptic receptor function. Bath application of GlcN+TMG resulted in a reduction in mIPSC amplitude (Fig 2Aii, cumulative probability distribution of amplitude, p<0.0001, KS D value = 0.24, Kolmogorov-Smirnov test; inset: p<0.0001, Wilcoxon matched-pairs signed rank test), but not inter-event interval (Fig 2Aiii, cumulative probability distribution of inter-event interval, p=0.96, KS D value = 0.032, Kolmogorov-Smirnov test; inset: p<0.0001, Wilcoxon matched-pairs signed rank test) in CA1 pyramidal cells. We observed a similar decrease in mIPSC amplitude in dentate GCs (Fig 2Bii, cumulative probability distribution, p<0.0001, KS D value = 0.12, Kolmogorov-Smirnov test; inset: p<0.0001, Wilcoxon matched-pairs signed rank test), but in contrast to CA1, we also observe a slight but significant increase in mISPC inter-event interval (Fig 2Biii, cumulative probability distribution, p<0.0001, KS D value = 0.099, Kolmogorov-Smirnov test; inset: p<0.0001, Wilcoxon matched-pairs signed rank test). However, the very small difference in mean values between control (373.5±7.3 ms) and GlcN+TMG (374.1±7.4 ms) suggests this significant difference may not be biologically relevant. Collectively, the decrease in mIPSC amplitude in the absence of a decrease in inter-event interval, at least in CA1 pyramical cells, is consistent with the interpretation that the dampening of inhibitory transmission following increased O-GlcNAcylation is due to a reduction in postsynaptic $GABA_AR$ function.

O-GlcNAcylation induces long-term depression of inhibitory transmission

We next tested if O-GlcNAcylation similarly affects the amplitude of electrically evoked IPSCs (eIPSCs), as evoked transmission may be dependent upon presynaptic vesicle pools (reviewed in Kavalali, 2015) distinct from those involved in spontaneous release. To address this and remaining questions, we focused our experiments on CA1 pyramidal cells. Following a 5 min stable baseline of eIPSCs (Cs Gluconate pipet solution; ECl- = -50 mV), bath applied GlcN+TMG elicited a significant reduction in eIPSC amplitude that lasted the duration of the recording (Fig 3 Ai and 3Aiii, p = 0.001, paired t-test).

We previously reported that a 10 min exposure to GlcN (5mM) alone induces a significant increase in O-GlcNAcylation in hippocampus that is readily reversed within a 10

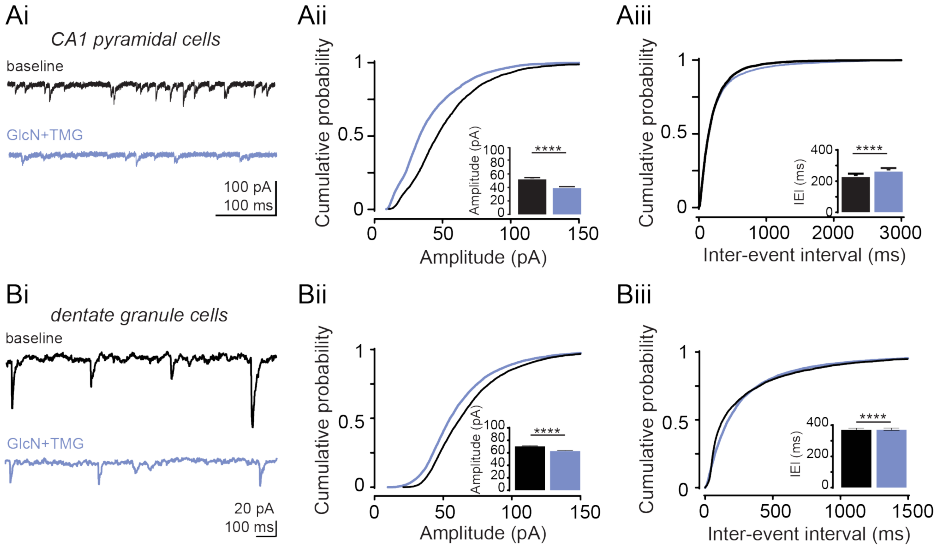

Figure 2: Acute increase in O-GlcNAcylation reduces miniature IPSC amplitude in hippocampal principal cells
(Ai) Representative mIPSC trace from CA1 pyramidal cell before (black) and after (blue) GlcN+TMG. (Aii) cumulative probability distribution of mIPSC amplitude (p<0.0001, KS D value = 0.24, Kolmogorov-Smirnov test); inset: average (± SEM) mIPSC amplitude. Baseline: 53.0±1.6 pA, GlcN+TMG: 40.0±1.0 pA (p<0.0001, Wilcoxon matched-pairs signed rank test, n=7 cells, 5 rats). (Aiii) Cumulative probability distribution of mIPSC IEI (p=0.96, KS D value = 0.032, Kolmogorov-Smirnov test); inset: average (± SEM) mIPSC IEI. Baseline: 236.7±14.3 ms vs GlcN+TMG: 271.5±16.2 ms (p=0.0005, Wilcoxon matched-pairs signed rank test, n=7 cells, 5 rats) (Bi) Representative mIPSC trace from dentate granule cell before (black) and after (blue) GlcN+TMG. (Bii) Cumulative probability distribution of mIPSC amplitude (p<0.0001, KS D value = 0.12, Kolmogorov-Smirnov test); inset: average (± SEM) mIPSC amplitude. Baseline: 71.1±0.4pA vs GlcN+TMG: 63.3±0.4 pA (p<0.0001, Wilcoxon matched-pairs signed rank test, n=12 cells, 6 rats). (Biii) Cumulative probability distribution of mIPSC IEI (p<0.0001, KS D value = 0.099, Kolmogorov-Smirnov test); inset: average (± SEM) mIPSC IEI. Baseline: 373.5±7.4 ms, GlcN+TMG: 368.8±7.5 ms (p=0.0005, Wilcoxon matched-pairs signed rank test, n=12 cells, 6 rats). ****p<0.0001.

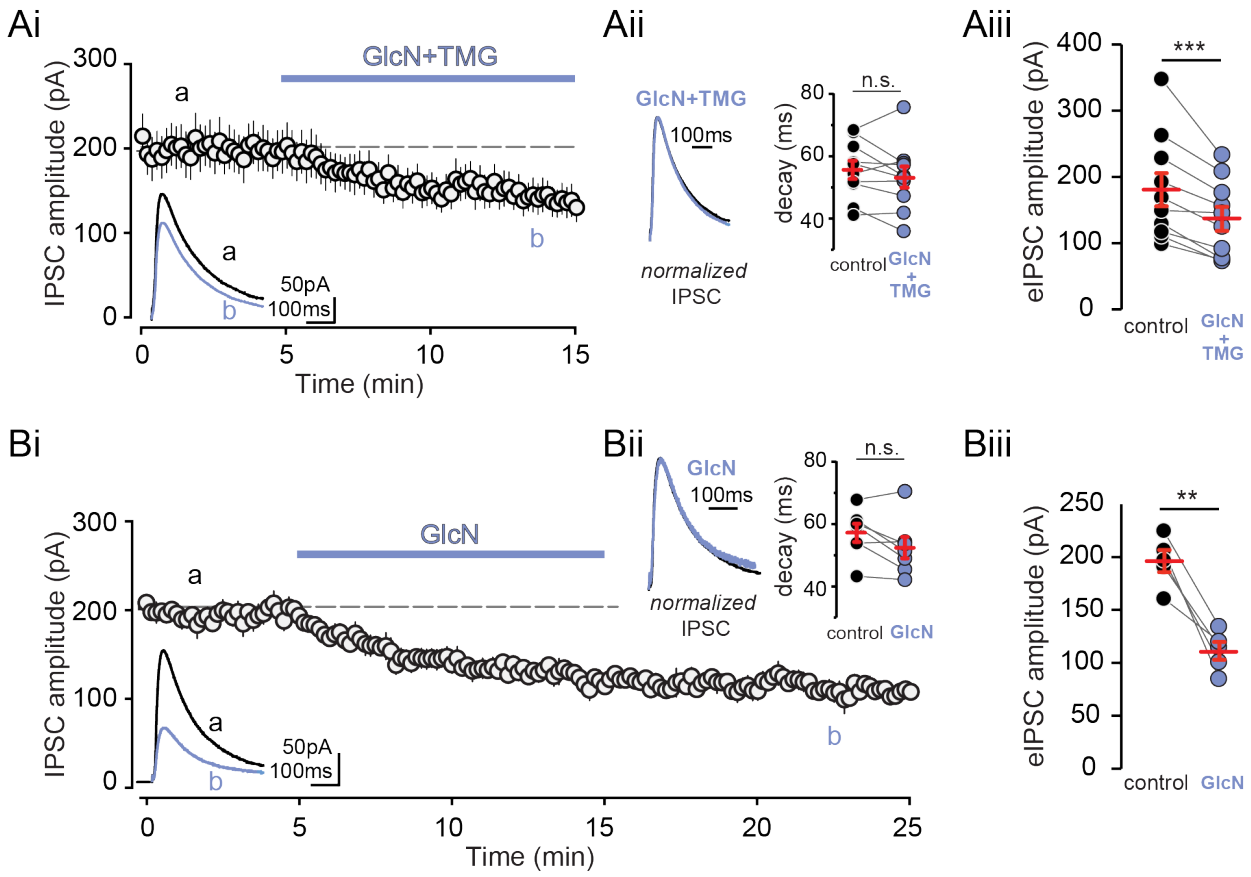

Figure 3: Increasing O-GlcNAcylation reduces evoked IPSC amplitude in CA1 pyramidal cells
(Ai) Group data showing average (±¬SEM) evoked IPSC (eIPSC) amplitude in control conditions and following GlcN+TMG wash on. Inset: representative eIPSC traces before (black) and after GlcN+TMG (blue). (Aii) (left) Normalized representative eIPSC traces and (right) decay time before (black) and after GlcN+TMG (blue). Red horizontal bars represent the mean ± SEM. control: 55.7±2.9 ms vs GlcN+TMG: 53.4±3.4 ms (p=0.23, paired-test, n=10 cells, 5 rats). (Aiii) eIPSC amplitudes before (black) and after (blue) GlcN+TMG. Red horizontal bars represent the mean ± SEM. control: 180.9±25.1 pA vs GlcN+TMG 136.7±18.3pA (p=0.001, paired-test, n=10 cells, 5 rats). (Bi) Group data showing average (±SEM) evoked IPSC amplitude in control conditions and following GlcN wash on and wash out. Inset: representative eIPSC traces before (black) and after GlcN (blue) wash out. (Bii) (left) Normalized representative eIPSC traces and (right) decay time before (black) and after (blue) GlcN wash out. Red horizontal bars represent the mean ± SEM. control: 57.1±2.9 ms vs GlcN: 52.4±3.5 ms. (p=0.06, paired-test, n=5 cells, 2 rats). (Biii) eIPSC amplitudes before (black) and after (blue) GlcN wash out. Red horizontal bars represent the mean ± SEM. control: 196.3±10.5 pA vs GlcN+TMG 111.4±8.4 pA (p=0.003, paired-test, n=5 cells, 2 rats). **p<0.01,****p<0.001.

min exposure to TMG (Taylor et al., 2014). Importantly, the depression of transmission at CA3-CA1 synapses induced by GlcN outlasted the transient increase in protein O-GlcNAcylation, demonstrating expression of a long-term depression (LTD) at these synapses (Taylor et al., 2014). To test if O-GlcNAcylation similarly causes long-term depression at GABAergic synapses onto CA1 pyramidal cells, we applied GlcN alone for 10 min and recorded eIPSCs for 10 min during washout and observed a persistent reduction in amplitude (Fig 3Bi and 3Biii, p = 0.003, paired t-test), consistent with expression of a form of LTD at GABAergic synapses.

O-GlcNAcylation biases E/I ratio towards excitation

Since O-GlcNAcylation induces LTD of both excitatory (Taylor et al., 2014) and inhibitory transmission onto CA1 pyramidal cells, we wondered what the overall effect of increased O-GlcNAc is on the balance of excitation to inhibition (E/I). Thus, we measured the E/I ratio at CA3-CA1 synapses by recording compound synaptic currents consisting of mono-synaptic EPSCs followed by di-synaptic IPSCs in whole-cell recordings of CA1 pyramidal cells voltage-clamped at -30 mV. We found that GlcN+TMG application caused a significant reduction in the IPSC component of the compound current (Fig 4Ai and 4Aii, open circles shown as %baseline current, p=0.007, paired t-test), with no significant change in the EPSC component (Fig 4Ai and 4Aii, closed circles shown as % baseline current, p=0.91, Wilcoxon matched-pairs signed rank test), indicating a stronger effect on synaptic inhibition versus excitation, and increasing the E/I ratio (Fig 4Aiii, p<0.05, paired t-test). We also confirmed the increase in the E/I ratio in current clamp recordings from CA1 pyramidal cells (Fig 4Biii, p<0.05, paired t-test).

These data show that an acute increase in O-GlcNAcylation causes a greater depression of the disynaptic $GABA_A$R-mediated IPSC/P than the mono-synaptic glutamatergic EPSC/P, thereby increasing the E/I ratio. Normally,

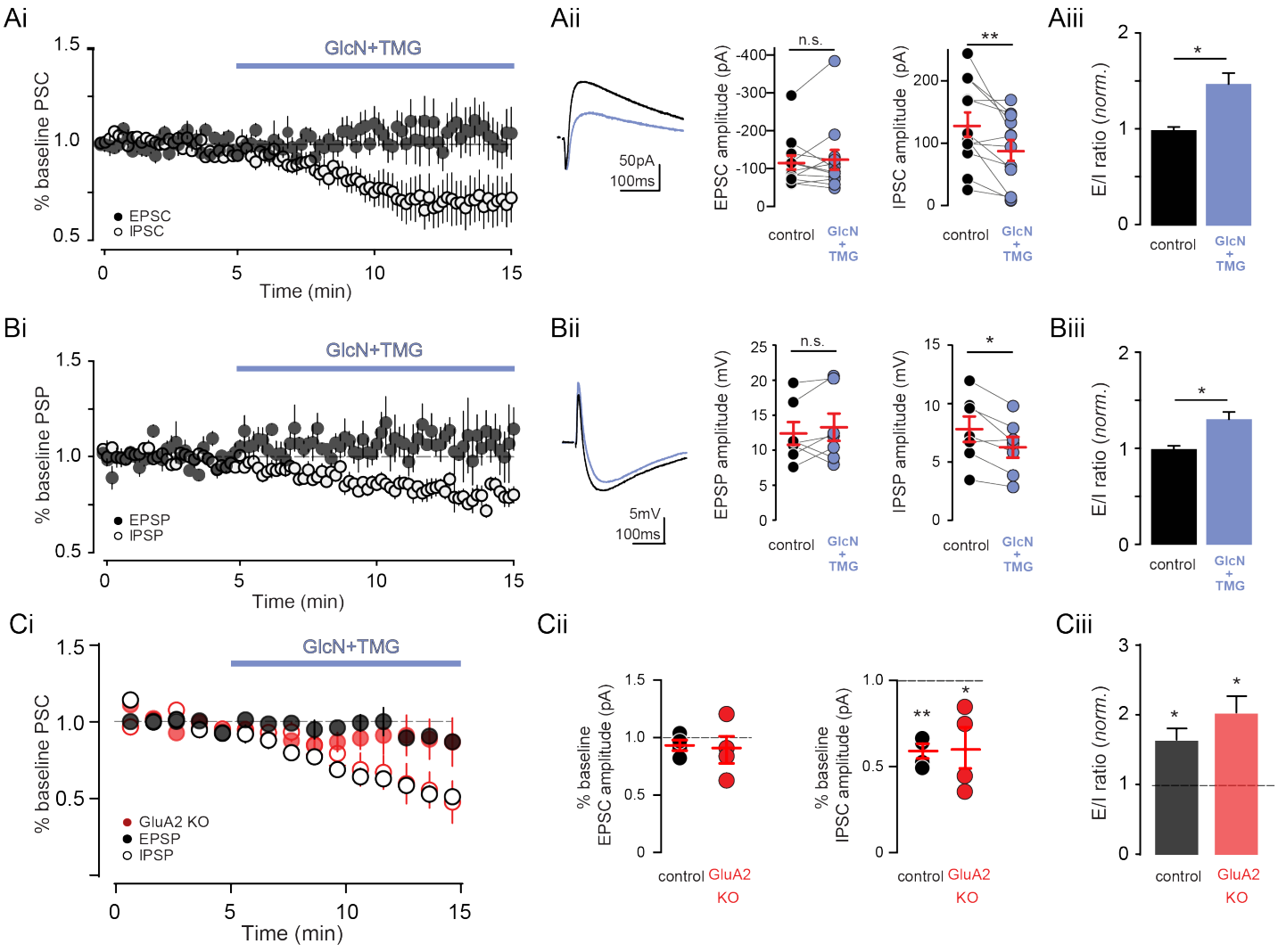

Figure 4: Increasing O-GlcNAcylation increases E- I ratio in pyramidal cells
(Ai) Normalized group data showing average (±SEM) evoked mono-synaptic EPSC (filled circles) and di-synaptic IPSC (open circles) amplitude in control conditions and following GlcN+TMG wash on. (Aii) (left) Representative compound EPSC and IPSC before (black) and after (blue) GlcN+TMG. (middle) EPSC amplitude before (black) and after (blue) GlcN+TMG. Red horizontal bars represent the mean ± SEM. control: -116.3±18.6 pA vs GlcN+TMG: -123.4±26.1 pA (p=0.91, Wilcoxon matched-pairs signed rank test, n=12 cells, 5 rats). (right) IPSC amplitude before (black) and after (blue) GlcN+TMG. Red horizontal bars represent the mean ± SEM. control: 130.2±19.5 pA vs GlcN+TMG: 88.7±16.6 pA (p=0.007, paired t-test, n=12 cells, 5 rats). (Aiii) Normalized E/I ratio after (blue) GlcN+TMG (p<0.05, test, paired t-test, n=12 cells, 5 rats) (Bi) Normalized group data showing average (±SEM) evoked mono-synaptic EPSP (filled circles) and di-synaptic IPSP (open circles) amplitude in control conditions and following GlcN+TMG wash on. (Bii) (left) Representative compound EPSP and IPSP before (black) and after (blue) GlcN+TMG. (middle) EPSP amplitude before (black) and after (blue) GlcN+TMG. Red horizontal bars represent the mean ± SEM. control: 12.3±1.6 mV vs GlcN+TMG: 13.2±1.9 mV (p=0.40, paired t-test, n=7 cells, 3 rats). (right) IPSP amplitude before (black) and after (blue) GlcN+TMG. Red horizontal bars represent the mean ± SEM. control: 7.8±1.1 mV vs GlcN+TMG: 6.2±0.9 mV (p=0.01, paired t-test, n=7 cells, 3 rats). (Biii) Normalized E/I ratio after (blue) GlcN+TMG (p<0.05, test, paired t-test, n=7 cells, 3 rats). (Ci) Normalized group data showing average (±SEM) evoked mono-synaptic EPSC (filled circles) and di-synaptic IPSC (open circles) amplitude in control (black) and GluA2 KO (red) before and following GlcN+TMG wash on. (Cii) (left) EPSC amplitude as percent of baseline after GlcN+TMG in control (black) and GluA2 KO (red). Red horizontal bars represent the mean ± SEM. (control: p=0.37, GluA2 KO: p=0.45, paired t-test, n=4 cells, 2 mice). (right) IPSC amplitude as percent of baseline after GlcN+TMG in control (black) and GluA2 KO (red). Red horizontal bars represent the mean ± SEM. (control: p=0.006, GluA2 KO: p=0.04, paired t-test, n=4 cells, 2 mice). Dotted lines represent normalized baseline EPSP/IPSP. (Ciii) E/I ratio after GlcN+TMG in control (black) and GluA2 KO (red). (control: p=0.03, GluA2 KO: p=0.02, paired t-test, n=4 cells, 2 mice). *p<0.05,**p<0.01.

$GABA_AR$-mediated transmission limits the amplitude of the excitatory EPSC/P through shunting the excitatory potential, and when the inhibitory shunt is decreased or blocked, the EPSC/P amplitude increases. Thus, decreasing the inhibitory shunt via the O-GlcNAc-mediated decrease in IPSC amplitude predicts that the EPSC/P amplitude should should increase (Mitchell and Silver, 2003), which we did not observe. We considered that the GluA2-AMPAR mediated O-GlcNAc LTD at CA3-CA1 synapses (Taylor et al., 2014), occurring in parallel with the decrease in IPSC amplitude could occlude the expected increase in EPSC/P amplitude. We directly tested this by recording compound

E-I currents in GluA2 knock-out (KO) mice in which the O-GlcNAc LTD at CA3-CA1 synapses should be absent. However, we continued to find that GlcN+TMG application increased the E/I ratio (Fig 4iii, p= 0.0208, paired t-test) and caused no significant change in the EPSC amplitude (Fig 4Ci, Fgenotype (1, 6) = 0.3820, p = 0.5592, two-way repeated measures ANOVA). Therefore, even when O-GlcNAc LTD is absent, decreasing shunting inhibition by increasing O-GlcNAcylation was not powerful enough to increase the EPSC amplitude.

O-GlcNAcylation reduces action potential probability in CA1 pyramidal cells

The increase in the E/I ratio predicts that synaptic drive should increase the probability that a subthreshold EPSP should become suprathreshold, and increase the probability of generating a synaptically driven action potential (AP) under conditions of elevated O-GlcNAc. Yet, this prediction is at odds with our previous study where we reported the opposite: increasing O-GlcNAc decreased basal spontaneous activity of CA3 pyramidal cells in an intact circuit, and depressed epileptic activity in area CA1 in hyperexcitable conditions generated by blocking $GABA_A$Rs (Stewart et al., 2017). Therefore, to determine the net effect of increasing protein O-GlcNAcylation on CA1 pyramidal cell output when the circuit is intact, we carried out current-clamp recordings from CA1 pyramidal cells and measured synaptically driven AP probability before and after application of GlcN+TMG. Stimulus intensity was set to achieve a ~25-50% success rate of generating a synaptically driven AP during the 5min ation caused a significant reduction in AP probability in all recorded cells, despite the increase in E/I ratio (Fig 5Aii and Aiii, p < 0.0001, paired t-test). Importantly, control experiments were interleaved to rule out technical artifacts since AP probability is particularly sensitive to any change in the quality of the recording (Fig 5Bi-Biii, p = 0.56, paired t-test).

As a further test of the effects of increasing O-GlcNAcylation on the net activity in the intact circuit, we performed a complementary experiment measuring the output of the CA1 population by recording extracellular population spikes (pSpike) in the CA1 pyramidal cell layer during a 10 min application of GlcN+TMG (Fig 5Ci, 10-15min). Consistent with the single-cell recordings, we observed a significant and sustained reduction in pSpike amplitude following an increase in O-GlcNAcylation (Fig 5Cii, p = 0.004, paired t-test), which supports our previous report of decreased CA3 output in the context of increased protein O-GlcNAcylation (Stewart et al., 2017).

Reduced intrinsic excitability of CA1 pyramidal cells contributes to the O-GlcNAc-mediated depression of excitability despite an increase in E/I ratio

The decrease in synaptically-evoked AP probability following increased O-GlcNAcylation despite increased E/I ratio

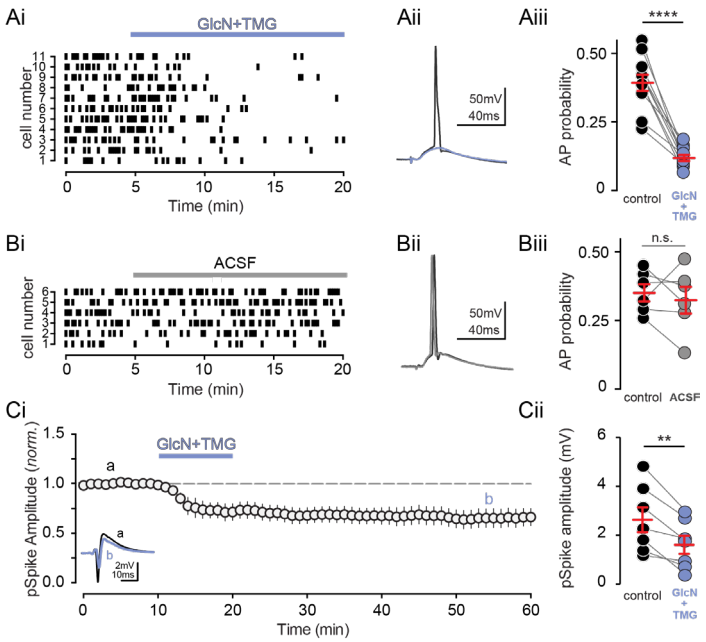

Figure 5: O-GlcNAcylation reduces CA1 action potential output
(Ai) Raster plot and (Aii) representative trace of synaptically-evoked APs before (black) and after GlcN+TMG (blue). (Aiii) AP probability before (black) and after (blue) GlcN+TMG. Red bars represent mean± SE. control: 0.39±0.03 vs. GlcN+TMG: 0.12±0.01 (p<0.0001, paired t-test, n=11 cells, 6 rats). (Bi) Raster plot and (Bii) representative average of synaptically-evoked APs before (black) and after (grey) ACSF application as a negative control. (Biii) Quantification of AP probability before (black) and after (grey) ACSF. Red bars represent mean ± SE. control: 0.35±0.03 vs. GlcN+TMG: 0.33±0.05 (p=0.5622, paired t-test, n=6 cells, 4 rats). (Ci) Normalized Group data showing pop-spike amplitude in baseline conditions and after GlcN+TMG (left) . inset: representative trace showing pop spike before (black) and after (blue) GlcN+TMG. (Cii) pSpike amplitude before (black) and after (blue) GlcN+TMG. Red bars represent mean ± SEM. control: 2.64±0.52 mV vs. GlcN+TMG: 1.61 ±0.38 mV (p=0.004, paired t-test, n=7 slices, 3 rats).**p<0.01, ****p<0.0001.

may arise as a consequence of non-mutually exclusive synaptic and intrinsic mechanisms. Therefore, we next tested the possibility that O-GlcNAcylation decreases intrinsic excitability by modulating the active and passive properties of CA1 pyramidal cells. We used whole-cell current clamp recordings of CA1 pyramidal cells during hyperpolarizing and depolarizing current injections in the presence of pharmacological blockers of $GABA_A$Rs, AMPARs, and NMDARs, to isolate the cells from synaptic inputs (Fig 6A). We found that O-GlcNAcylation caused a significant reduction in the input resistance (Fig 6C, p=0.031, paired t-test) when cells were isolated from the synaptic network, and a significant increase in rheobase, or the minimum current required to elicit a single action potential (Fig 6D, p=0.036, paired t-test). We also observed an increase in AP threshold (Fig 6E, p=0.030, paired t-test), but no difference in AP shape (Fig 6F, 6G, 6H, AP amplitude: p=0.441; AP rise: p=0.143; AP half width: p=0.653, paired t-test). Additionally, we found a small but significant decrease in the number of action potentials generated with higher current injection steps following GlcN+TMG application (FO-GlcNAc(1,8)= 5.81, p<0.05, two-way repeated measures ANOVA). These changes are

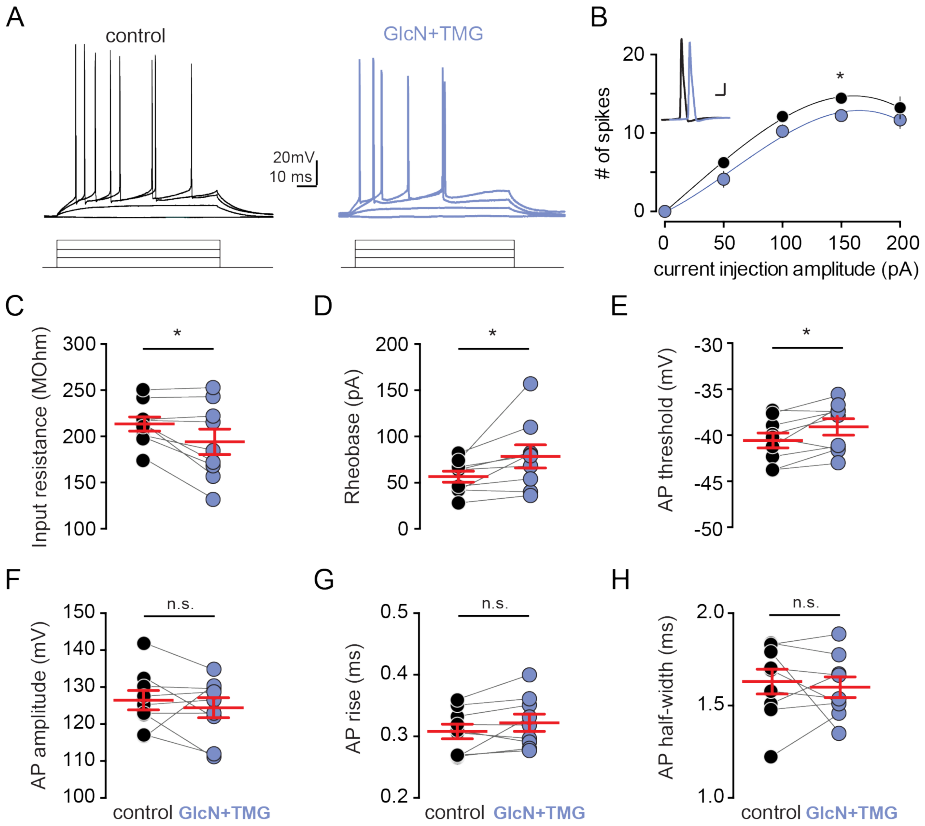

Figure 6: O-GlcNAcylation reduces CA1 action potential output
(Ai) Raster plot and (Aii) representative trace of synaptically-evoked APs before (black) and after GlcN+TMG (blue). (Aiii) AP probability before (black) and after (blue) GlcN+TMG. Red bars represent mean± SE. control: 0.39±0.03 vs. GlcN+TMG: 0.12±0.01 ($p<0.0001$, paired t-test, n=11 cells, 3 rats). (Bi) Raster plot and (Bii) representative average of synaptically-evoked APs before (black) and after (grey) ACSF application as a negative control. (Biii) Quantification of AP probability before (black) and after (grey) ACSF. Red bars represent mean ± SE. control: 0.35±0.03 vs. GlcN+TMG: 0.33±0.05 ($p=0.5622$, paired t-test, n=6 cells, X rats). (Ci) Normalized Group data showing pop-spike amplitude in baseline conditions and after GlcN+TMG (left) . inset: representative trace showing pop spike before (black) and after (blue) GlcN+TMG. (Cii) pSpike amplitude before (black) and after (blue) GlcN+TMG. Red bars represent mean ± SEM. control: 2.64±0.52 mV vs. GlcN+TMG: 1.61 ±0.38 mV ($p=0.004$, paired t-test, n=7 slices, X rats).**$p<0.01$, ****$p<0.0001$.

consistent with a decrease in intrinsic excitability.

Collectively, our current and previously published data suggest that both synaptic and intrinsic mechanisms contribute to a net decrease in CA1 pyramidal cell excitability, despite a larger O-GlcNAc-mediated depression of inhibitory versus excitatory transmission, which increases the E/I ratio. Therefore, to distinguish the decreased intrinsic excitability from the synaptic depression, we repeated the pSpike recordings in GluA2 KO mice in which O-GlcNAc LTD at CA3-CA1 synapses will be absent (Fig 7Ai and 7Aii). Interestingly, increasing O-GlcNAcylation depressed pSpike amplitude in both the wild-type and GluA2 KO mice (Fig 7Aiii, control: $p<0.01$ KO: $p<0.01$, sidak's multiple comparisons test), while the persistent depression (O-GlcNAc LTD) following GlcN+TMG wash-out was only observed in wild-type mice, as expected (Fig 7Aiii, control: $p<0.01$ KO: $p>0.05$, sidak's multiple comparison test). Thus, the early depression of the pSpike amplitude during GlcN+TMG application is likely a consequence of decreasing CA1 pyramidal cell intrinsic excitability, while the persistent depression of excitability is a consequence of synaptic depression mediated by O-GlcNAc LTD.

Discussion

We provide, for the first time, empirical evidence of a role for protein O-GlcNAcylation in regulating synaptic inhibition in principal cells of the hippocampus. First, we show that acutely increasing O-GlcNAcylation reduces the frequency and magnitude of spontaneous-IPSCs in CA1 pyramidal cells and dentate granule cells, and selectively decreases the amplitude of mini-IPSCs, suggesting a postsynaptic mechanism. The amplitude of evoked-IPSCs onto CA1 pyramidal cells is similarly reduced, and the depression is long-lasting, suggesting a form of LTD induced by O-GlcNAc at GABAergic synapses. In a hippocampal circuit with intact excitation and inhibition, an acute increase in O-GlcNAcylation reduces the strength of inhibition while seemingly leaving excitation intact. The greater effect on inhibition versus excitation predicts an overall increase in excitability. Surprisingly, we show that O-GlcNAcylation modulates the final output of CA1 pyramidal cells by reducing the action potential probability through intrinsic and synaptic mechanisms. These results position protein O-GlcNAcylation as a potent regulator of both synaptic inhibition as well as excitation, as we reported previously (Stewart et al., 2017;

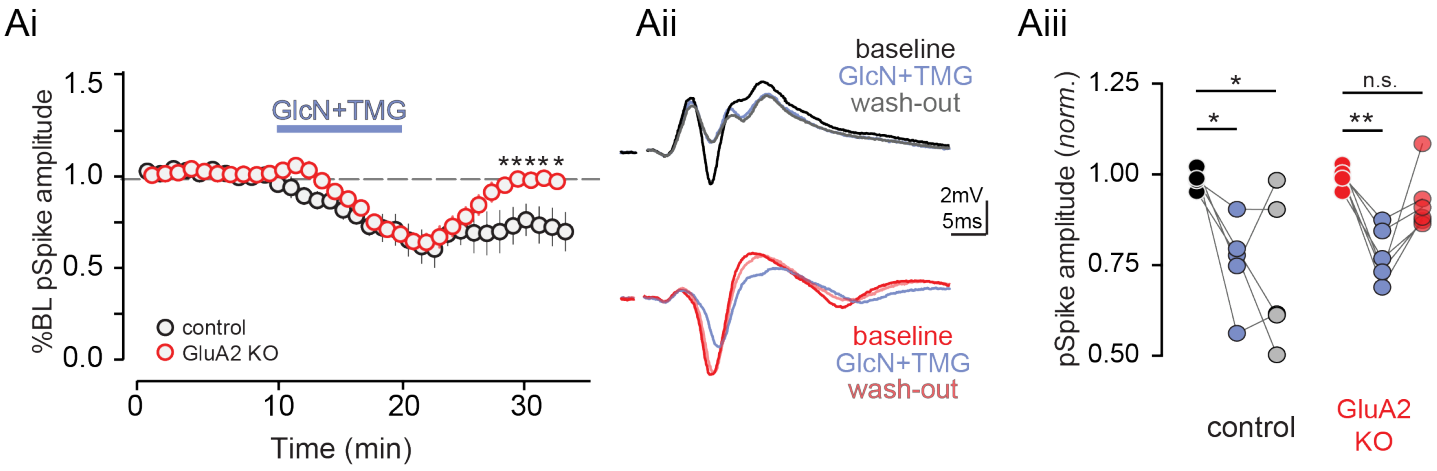

Figure 7: Increased O-GlcNAcylation reduces CA1 spike output
(Ai) Normalized group data showing pop-spike amplitude in baseline conditions and after GlcN+TMG in control (black) and GluA2 KO (red) mice (*p<0.05, two-way ANOVA with Sidak's multiple comparison test, n= 5 slices, 2 rats). (Aii) Representative averaged traces showing (top) pop spike amplitude before (black), after (blue) GlcN+TMG, and following wash-out (grey) in control mice and (bottom) pop spike amplitude before (red), after (blue) GlcN+TMG and following wash-out (pink) in GluA2 KO mice. (Aiii) Pop spike amplitude before (black), after (blue) GlcN+TMG and following wash-out (grey) in control mice (baseline vs. GlcN+TMG: p<0.05; baseline vs. wash-out: p<0.05, repeated measures one-way ANOVA with Sidak's multiple comparison's test, n= 5 slices, 2 rats) and pop spike amplitude before (red), after (blue) GlcN+TMG, and following wash-out (pink) in GluA2 KO mice (baseline vs. GlcN+TMG: p<0.01; baseline vs. wash-out: p>0.05, repeated measures one-way ANOVA with Sidak's multiple comparison's test, n= 5 slices, 2 rats). *p<0.05, **p<0.01.

Taylor et al., 2014).

While the effect of the analogous post translational modification, phosphorylation, on synaptic transmission has been extensively characterized, little is known about the role of O-GlcNAcylation on excitatory and inhibitory transmission. The post-translational O-linked addition of N-acetyl glucosamine to proteins is a dynamic process catalyzed by the enzymes OGT and OGA, which are highly expressed particularly in the hippocampus and cerebellum in the brain (Liu et al., 2004b). We have previously shown that acute increases in O-GlcNAcylation causes a GluA2 AMPAR subunit dependent long-term depression of excitatory transmission (termed O-GlcNAc LTD) in CA1 pyramidal cell dendritic field potentials and CA1 populations spikes (Stewart et al., 2017; Taylor et al., 2014). Here, we report that an acute increase in protein O-GlcNAcylation similarly causes a depression of global inhibition onto CA1 pyramidal cells and dentate granule cells. This includes a reduction in the amplitude but not frequency of mini-IPSCs onto hippocampal principal cells, suggesting a post-synaptic site of action. This reduction in inhibition could involve a number of mechanisms including internalization of $GABA_A$Rs, a change in the conductance of individual $GABA_A$Rs, or destabilization of scaffolding proteins that anchor $GABA_A$Rs to the membrane. Indeed, recent work (Hwang and Rhim, 2019) suggests the reduction in mini-EPSC amplitude following increased O-GlcNAcylation involves the endocytosis of GluA2 subunit containing AMPARs, which likely explains expression of the GluA2-dependent LTD we previously reported (Taylor et al., 2014). Additionally, phosphorylation of specific serine/threonine residues on $GABA_A$Rs modulates inhibitory transmission, an effect that includes a reduction in $GABA_A$R currents (Nakamura et al., 2015), which might also occur following increased O-GlcNAc.

Notably, phosphorylation alters inhibition in the brain in a kinase- and region-specific manner (for review, see Nakamura et al., 2015)). Activation of PKA depresses synaptic $GABA_A$R function in CA1 pyramidal cells but not dentate gyrus granule cells (GCs), whereas PKC activation alters mini-IPSC amplitude in GCs alone (Poisbeau et al., 1999). O-GlcNAcylation, however, is uniquely positioned to turn down global inhibition in a non region-specific manner as only one enzyme, OGT, is known to catalyze its addition to proteins. While phosphorylation and O-GlcNAcylation on some proteins can occlude one another (Cheng et al., 2000; Chou et al., 1995; Dias et al., 2009; Griffith and Schmitz, 1999; Liu et al., 2004a), oher times they can act independently (Taylor et al., 2014) or synergistically (for review, see Zeidan and Hart, 2010) . Whether there is a negative or positive interplay between the effects of phosphorylation and O-GlcNAcylation on inhibition remains to be determined.

We show that O-GlcNAcylation depresses the di-synaptic IPSC while leaving the mono-synaptic EPSC intact following CA3 axon stimulation stimulation. However, this increase in the E/I ratio leads to a counterintuitive decrease in the synaptically-evoked action potential probability in pyramidal cells. While subthreshold EPSPs can spatially and temporally summate to generate APs, the efficacy of EPSP

to spike coupling is thought to depend on several factors including IPSP magnitude and timing (Pouille and Scanziani, 2001), as well as passive and active properties of the post-synaptic neuron (Magee, 2000). Interestingly, (i) individual pyramidal cells vary widely in their threshold afferent stimulation required for spiking, but this threshold is controlled by the magnitude of the EPSC and not the amplitude or timing of inhibition (Pouille et al., 2009); and (ii) increasing O-GlcNAcylation leads to a depression of field EPSPs in area CA1, likely owing to an internalization of GluA2 containing AMPARs (Hwang and Rhim, 2019; Stewart et al., 2017). Thus, it stands to reason that the decrease in AP probability despite the increase in E/I ratio following increased O-GlcNAcylation could stem from a concomitant depression of the CA3-CA1 EPSC. We found that O-GlcNAcylation not only reduces the AMPAR mediated dendritic depolarization (Taylor et al., 2014), but also changes the intrinsic properties of CA1 neurons, making it harder for the cell to spike. This change in intrinsic properties following an increase in O-GlcNAc is consistent with recently published work by Hwang and Rhim, 2019) showing a reduction in depolarizing voltage-gated sodium channel currents and an increase in hyperpolarizing voltage-gated potassium currents. We have also previously reported a reduction in basal spontaneous spiking activity in area CA3 of hippocampus following increased O-GlcNAc (Stewart et al., 2017), further supporting a suppressive effect of O-GlcNAcylation on neuronal output. Notably, this finding is contrary to studies using genetic strategies to increase O-GlcNAcylation (Yang et al., 2017), which reported no changes in intrinsic excitability, or mini-EPSCs and -IPSCs following heterozygous loss of function mutation of OGA, whose protein product catalyzes the removal of O-GlcNAc from proteins. The conflicting results are mostly likely due to differential effects of acute versus chronic upregulation in protein O-GlcNAcylation, as chronic changes can produce compensatory mechanisms to maintain synaptic function.

Studying the effect of acute, moment-to-moment changes in O-GlcNAc levels on synaptic transmission likely reflects the impact of metabolically driven changes in O-GlcNAcylation occurring in vivo. The OGT substrate UDP-GlcNAc is produced by the flux of glucose through the hexosamine biosynthetic pathway, which incorporates nucleotides, fatty acids, and amino acids. For instance, fasting promotes energy conservation via the upregulation of OGT and O-GlcNAc and its effect on the activity of hypothalamic neurons (Ruan et al., 2014). Conversely, chronic elevation of glu cose can also increase O-GlcNAcylation of certain targets, contributing to cardiac and neuronal pathophysiology (Erickson et al., 2013). As such, O-GlcNAcylation is positioned to operate as a nutrient sensor (for review, see Lagerlöf, 2018). Additionally, O-GlcNAcylation plays a crucial role in pathological states such as diabetes (Erickson et al., 2013; Vaidyanathan and Wells, 2014) where its elevation can contribute to disease pathogenesis, in epilepsy where increasing O-GlcNAc is protective (Sánchez et al., 2019; Stewart et al., 2017), and in neurodegeneration (Levine etal., 2019; Wang et al., 2016; Yuzwa and Vocadlo, 2014; Yuzwa et al., 2008, 2012, 2014a, 2014b; Zhu et al., 2014), where increasing O-GlcNAc can decrease pathological accumulation of phosphorylated tau or α-synuclein. Collectively, studies published by us and others suggest that maintaining proper balance in O-GlcNAcylation is critical to maintaining normal hippocampal function, as too much or too little O-GlcNAc has been linked to deficits in learning and memory (Taylor et al 2014; Yang et al 2017; Wang et al 2016). Revealing the complex changes in neuronal and synaptic function induced by alterations in O-GlcNAcylation in non-pathological and pathological states will require further investigation.

Acknowledgements

This research was supported by NIH NINDS RO1NS076312 (L.L.M and J.C.) ,1F31NS095568 (L.T.S), and an Alabama State funded Graduate Research Scholars Program Fellowship (KA).

Declaration of Interest

The authors declare no competing financial interests.

References

Cheng, X., Cole, R.N., Zaia, J., and Hart, G.W. (2000). Al ternative O-Glycosylation/O-Phosphorylation of the Murine Estrogen Receptor β. Biochemistry 39, 11609–11620.

Chou, T.Y., Hart, G.W., and Dang, C.V. (1995). c-Myc is glycosylated at threonine 58, a known phosphorylation site and a mutational hot spot in lymphomas. J. Biol. Chem. 270, 18961–18965.

Dias, W.B., Cheung, W.D., Wang, Z., and Hart, G.W. (2009). Regulation of calcium/calmodulin-dependent kinase IV by O-GlcNAc modification. J. Biol. Chem. 284, 21327–21337.

Erickson, J.R., Pereira, L., Wang, L., Han, G., Ferguson, A., Dao, K., Copeland, R.J., Despa, F., Hart, G.W., Ripplinger, C.M., et al. (2013). Diabetic hyperglycaemia activates CaMKII and arrhythmias by O-linked glycosylation. Nature 502, 372–376.

Farrant, M., and Nusser, Z. (2005). Variations on an inhibitory theme: phasic and tonic activation of GABA(A) receptors. Nat. Rev. Neurosci. 6, 215–229.

Fernandez, F., Morishita, W., Zuniga, E., Nguyen, J., Blank, M., Malenka, R.C., and Garner, C.C. (2007). Pharmacotherapy for cognitive impairment in a mouse model of Down syndrome. Nat. Neurosci. 10, 411–413.

Gogolla, N., Leblanc, J.J., Quast, K.B., Südhof, T.C., Fagiolini, M., and Hensch, T.K. (2009). Common circuit defect of excitatory-inhibitory balance in mouse models of autism. J. Neurodev. Disord. 1, 172–181.

Griffith, L.S., and Schmitz, B. (1999). O-linked N-acetylglucosamine levels in cerebellar neurons respond reciprocally

to pertubations of phosphorylation. Eur. J. Biochem. 262, 824–831.

Hwang, H., and Rhim, H. (2019). Acutely elevated O-GlcNAcylation suppresses hippocampal activity by modulating both intrinsic and synaptic excitability factors. Sci. Rep. 9, 7287.

Kavalali, E.T. (2015). The mechanisms and functions of spontaneous neurotransmitter release. Nat. Rev. Neurosci. 16, 5–16.

Keembiyehetty, C., Love, D.C., Harwood, K.R., Gavrilova, O., Comly, M.E., and Hanover, J.A. (2015). Conditional knock-out reveals a requirement for O-linked N-Acetylglucosaminase (O-GlcNAcase) in metabolic homeostasis. J. Biol. Chem. 290, 7097–7113.

Kehrer, C., Maziashvili, N., Dugladze, T., and Gloveli, T. (2008). Altered Excitatory-Inhibitory Balance in the NMDA-Hypofunction Model of Schizophrenia. Front. Mol. Neurosci. 1, 6.

Keller, C.A., Yuan, X., Panzanelli, P., Martin, M.L., Alldred, M., Sassoè-Pognetto, M., and Lüscher, B. (2004). The gamma2 subunit of GABA(A) receptors is a substrate for palmitoylation by GODZ. J. Neurosci. 24, 5881–5891.

Kreppel, L.K., Blomberg, M.A., and Hart, G.W. (1997). Dynamic glycosylation of nuclear and cytosolic proteins. Cloning and characterization of a unique O-GlcNAc transferase with multiple tetratricopeptide repeats. J. Biol. Chem. 272, 9308–9315.

Lagerlöf, O. (2018). O-GlcNAc cycling in the developing, adult and geriatric brain. J Bioenerg Biomembr 50, 241–261.

Lagerlöf, O., Slocomb, J.E., Hong, I., Aponte, Y., Blackshaw, S., Hart, G.W., and Huganir, R.L. (2016). The nutrient sensor OGT in PVN neurons regulates feeding. Science 351, 1293–1296.

Lagerlöf, O., Hart, G.W., and Huganir, R.L. (2017). O-GlcNAc transferase regulates excitatory synapse maturity. Proc. Natl. Acad. Sci. USA 114, 1684–1689.

Levine, P.M., Galesic, A., Balana, A.T., Mahul-Mellier, A.-L., Navarro, M.X., De Leon, C.A., Lashuel, H.A., and Pratt, M.R. (2019). α-Synuclein O-GlcNAcylation alters aggregation and toxicity, revealing certain residues as potential inhibitors of Parkinson's disease. Proc. Natl. Acad. Sci. USA 116, 1511–1519.

Liu, F., Iqbal, K., Grundke-Iqbal, I., Hart, G.W., and Gong, C.-X. (2004a). O-GlcNAcylation regulates phosphorylation of tau: a mechanism involved in Alzheimer's disease. Proc. Natl. Acad. Sci. USA 101, 10804–10809.

Liu, K., Paterson, A.J., Zhang, F., McAndrew, J., Fukuchi, K.-I., Wyss, J.M., Peng, L., Hu, Y., and Kudlow, J.E. (2004b). Accumulation of protein O-GlcNAc modification inhibits proteasomes in the brain and coincides with neuronal apoptosis in brain areas with high O-GlcNAc metabolism. J. Neurochem. 89, 1044–1055.

Magee, J.C. (2000). Dendritic integration of excitatory synaptic input. Nat. Rev. Neurosci. 1, 181–190.

McDonald, B.J., and Moss, S.J. (1997). Conserved phosphorylation of the intracellular domains of GABA(A) receptor beta2 and beta3 subunits by cAMP-dependent protein kinase, cGMP-dependent protein kinase protein kinase C and Ca2+/calmodulin type II-dependent protein kinase. Neuropharmacology 36, 1377–1385.

Nakamura, Y., Darnieder, L.M., Deeb, T.Z., and Moss, S.J. (2015). Regulation of GABAARs by phosphorylation. Adv. Pharmacol. 72, 97–146.

Poisbeau, P., Cheney, M.C., Browning, M.D., and Mody, I. (1999). Modulation of synaptic GABAA receptor function by PKA and PKC in adult hippocampal neurons. J. Neurosci. 19, 674–683.

Pouille, F., and Scanziani, M. (2001). Enforcement of temporal fidelity in pyramidal cells by somatic feed-forward inhibition. Science 293, 1159–1163.

Pouille, F., Marin-Burgin, A., Adesnik, H., Atallah, B.V., and Scanziani, M. (2009). Input normalization by global feedforward inhibition expands cortical dynamic range. Nat. Neurosci. 12, 1577–1585.

Rathenberg, J., Kittler, J.T., and Moss, S.J. (2004). Palmitoylation regulates the clustering and cell surface stability of GABAA receptors. Mol. Cell. Neurosci. 26, 251–257.

Roberson, E.D., Halabisky, B., Yoo, J.W., Yao, J., Chin, J., Yan, F., Wu, T., Hamto, P., Devidze, N., Yu, G.-Q., et al. (2011). Amyloid-β/Fyn-induced synaptic, network, and cognitive impairments depend on tau levels in multiple mouse models of Alzheimer's disease. J. Neurosci. 31, 700–711.

Ruan, H.-B., Dietrich, M.O., Liu, Z.-W., Zimmer, M.R., Li, M.-D., Singh, J.P., Zhang, K., Yin, R., Wu, J., Horvath, T.L., et al. (2014). O-GlcNAc transferase enables AgRP neurons to suppress browning of white fat. Cell 159, 306–317.

Saliba, R.S., Michels, G., Jacob, T.C., Pangalos, M.N., and Moss, S.J. (2007). Activity-dependent ubiquitination of GABA(A) receptors regulates their accumulation at synaptic sites. J. Neurosci. 27, 13341–13351.

Sánchez, R.G., Parrish, R.R., Rich, M., Webb, W.M., Lockhart, R.M., Nakao, K., Ianov, L., Buckingham, S.C., Broadwater, D.R., Jenkins, A., et al. (2019). Human and rodent temporal lobe epilepsy is characterized by changes in O-GlcNAc homeostasis that can be reversed to dampen epileptiform activity. Neurobiol. Dis. 124, 531–543.

Shafi, R., Iyer, S.P., Ellies, L.G., O'Donnell, N., Marek, K.W., Chui, D., Hart, G.W., and Marth, J.D. (2000). The O-GlcNAc transferase gene resides on the X chromosome and is essential for embryonic stem cell viability and mouse ontogeny. Proc. Natl. Acad. Sci. USA 97, 5735–5739.

Stewart, L.T., Khan, A.U., Wang, K., Pizarro, D., Pati, S., Buckingham, S.C., Olsen, M.L., Chatham, J.C., and McMahon, L.L. (2017). Acute Increases in Protein O-GlcNAcylation Dampen Epileptiform Activity in Hippocampus. J. Neurosci. 37, 8207–8215.

Taylor, E.W., Wang, K., Nelson, A.R., Bredemann, T.M.,

Fraser, K.B., Clinton, S.M., Puckett, R., Marchase, R.B., Chatham, J.C., and McMahon, L.L. (2014). O-GlcNAcylation of AMPA receptor GluA2 is associated with a novel form of long-term depression at hippocampal synapses. J. Neurosci. 34, 10–21.

Trinidad, J.C., Barkan, D.T., Gulledge, B.F., Thalhammer, A., Sali, A., Schoepfer, R., and Burlingame, A.L. (2012). Global identification and characterization of both O-GlcNAcylation and phosphorylation at the murine synapse. Mol. Cell Proteomics 11, 215–229.

Vaidyanathan, K., and Wells, L. (2014). Multiple tissue-specific roles for the O-GlcNAc post-translational modification in the induction of and complications arising from type II diabetes. J. Biol. Chem. 289, 34466–34471.

Vithlani, M., Terunuma, M., and Moss, S.J. (2011). The dynamic modulation of GABA(A) receptor trafficking and its role in regulating the plasticity of inhibitory synapses. Physiol. Rev. 91, 1009–1022.

Wang, A.C., Jensen, E.H., Rexach, J.E., Vinters, H.V., and Hsieh-Wilson, L.C. (2016). Loss of O-GlcNAc glycosylation in forebrain excitatory neurons induces neurodegeneration. Prim, S.-J., Yoon, S., Hur, J.-H., Park, J.-I., Lee, C., Nam, D., et al. (2017). Memory and synaptic plasticity are impaired by dysregulated hippocampal O-GlcNAcylation. Sci. Rep. 7, 44921.

Yuzwa, S.A., and Vocadlo, D.J. (2014). O-GlcNAc and neurodegeneration: biochemical mechanisms and potential roles in Alzheimer's disease and beyond. Chem. Soc. Rev. 43, 6839–6858.Proc. Natl. Acad. Sci. USA 113, 15120–15125.

Yang, X., and Qian, K. (2017). Protein O-GlcNAcylation: emerging mechanisms and functions. Nat. Rev. Mol. Cell Biol. 18, 452–465.

Yang, Y.R., Song, S., Hwang, H., Jung, J.H., Kim, S.-J., Yoon, S., Hur, J.-H., Park, J.-I., Lee, C., Nam, D., et al. (2017). Memory and synaptic plasticity are impaired by dysregulated hippocampal O-GlcNAcylation. Sci. Rep. 7, 44921.

Yuzwa, S.A., Macauley, M.S., Heinonen, J.E., Shan, X., Dennis, R.J., He, Y., Whitworth, G.E., Stubbs, K.A., McEachern, E.J., Davies, G.J., et al. (2008). A potent mechanism-inspired O-GlcNAcase inhibitor that blocks phosphorylation of tau in vivo. Nat. Chem. Biol. 4, 483–490.

Yuzwa, S.A., Shan, X., Macauley, M.S., Clark, T., Skorobogatko, Y., Vosseller, K., and Vocadlo, D.J. (2012). Increasing O-GlcNAc slows neurodegeneration and stabilizes tau against aggregation. Nat. Chem. Biol. 8, 393–399.

Yuzwa, S.A., Cheung, A.H., Okon, M., McIntosh, L.P., and Vocadlo, D.J. (2014a). O-GlcNAc modification of tau directly inhibits its aggregation without perturbing the conformational properties of tau monomers. J. Mol. Biol. 426, 1736–1752.

Yuzwa, S.A., Shan, X., Jones, B.A., Zhao, G., Woodward, M.L., Li, X., Zhu, Y., McEachern, E.J., Silverman, M.A., Watson, N.V., et al. (2014b). Pharmacological inhibition of O-GlcNAcase (OGA) prevents cognitive decline and amyloid plaque formation in bigenic tau/APP mutant mice. Mol. Neurodegener. 9, 42.

Zeidan, Q., and Hart, G.W. (2010). The intersections between O-GlcNAcylation and phosphorylation: implications for multiple signaling pathways. J. Cell Sci. 123, 13–22.

Zhu, Y., Shan, X., Yuzwa, S.A., and Vocadlo, D.J. (2014). The emerging link between O-GlcNAc and Alzheimer disease. J. Biol. Chem. 289, 34472–34481.

Materials and methods

All experimental procedures were approved by the University of Alabama at Birmingham Institutional Animal Care and Use Committee and follow the National Institutes of Health experimental guidelines.

Hippocampal slice preparation. Male and female Sprague Dawley rats (age 4-8 weeks; Charles River Laboratories) or male and female mice (age 4 – 12 weeks, GluA2 KO, Jax Labs #002913) were anesthetized with isoflurane, rapidly decapitated, and brains removed; 400μm (rats) or 350 μm (mice) coronal slices from dorsal hippocampus wereprepared on a VT1000P vibratome (Leica Biosystems) in oxygenated (95%O2/5%CO2) ice-cold, high sucrose cutting solution (in mM as follows: 85.0 NaCl, 2.5 KCl, 4.0 MgSO4, 0.5 CaCl2, 1.25 NaPO4, 25.0 glucose, 75.0 sucrose). After cutting, slices were held at room temperature for 1 to 5 hr in a submersion chamber with continuously oxygenated standard ACSF (in mM as follows: 119.0 NaCl, 2.5 KCl, 1.3 MgSO4, 2.5 CaCl2, 1.0 NaH2PO4, 26.0 NaHCO3, 11.0 glucose) with 2mM kynurenic acid to better preserve slice health.

Electrophysiology. All recordings were performed in a submersion chamber with continuous perfusion of oxygenated standard ACSF. The blind patch technique was used to acquire whole-cell recordings from CA1 pyramidal neurons and dentate granule cells (GCs). Neuronal activity was recorded using an Axopatch 200B amplifier and pClamp10 acquisition software (Molecular Devices, Sunnyvale, CA). Signals were filtered at 5 kHz and digitized at 10 kHz (Digidata 1440). Patch pipettes (BF150-086 or BF150-110; Sutter Instruments, Novato, CA) were pulled on a Sutter P-97 (Sutter Instruments, Novato, CA) horizontal puller to a resistance between 2-6 MΩ. Spontaneous inhibitory postsynaptic currents (sIPSCs) were pharmacologically isolated with bath perfusion of DNQX (10μM; Sigma) and DL-AP5 (50μM; Tocris) or R-CPP (5 μM; Abcam). Purity of GABAAR currents was verified with perfusion of picrotoxin (50μM; Sigma) following experimental recording. Spontaneous and miniature IPSCs were recorded using CsCl internal solution (in mM: 140.0 CsCl, 10.0 EGTA, 5.0 MgCl2, 2.0 Na-ATP, 0.3 Na-GTP, 10.0 HEPES; ECl = 0mV). Evoked GABAAR currents were recorded using Cs-gluconate internal solution (in mM: 100.0 Cs-gluconate, 0.6 EGTA, 5.0 MgCl2, 2.0 Na-ATP, 0.3 Na-GTP, 40.0 HEPES; ECl = -61.5 mV) with a

twisted nichrome wire bipolar electrode positioned in stratum radiatum (100µs, 0.1Hz). Whole-cell current clamp recordings from CA1 pyramidal neurons were carried out using K-gluconate internal solution (in mM: 120.0 K-gluconate, 0.6 EGTA, 5.0 MgCl2, 2.0 Na-ATP, 0.3 Na-GTP, 20.0 HEPES; ECl = -61.5 mV). All cells were dialized for 3-7min prior to the beginning of experimental recordings. Stability of series resistance was verified using post-hoc scaling of averaged waveforms before and after pharmacologicaly increasing O-GlcNAcylation. pSpikes in the CA1 cell body layer were evoked by stimulating Schaffer collaterals with pairs of pulses (0.1 Hz, 100 µs duration at 50 ms interval) in stratum radiatum with a twisted nichrome wire bipolar electrode and recorded with a glass pipet filled with aCSF placed nearby in stratum pyramidale.

Modulation of O-GlcNAc levels. As previously described (Taylor et al., 2014; Stewart et al., 2017), O-GlcNAcylation was acutely increased via bath application of glucosamine (GlcN, 5 mM; Sigma) alone or in combination with the selec potent OGA inhibitor (Ki = 21 nM; human OGA) currently available (Macauley et al., 2005; Yuzwa et al., 2008). GlcN and TMG were used in combination to ensure robust and lasting increases in protein O-GlcNAc levels. In some some etive OGA inhibitor TMG (1 µM; Chem Molecules), the most xperiments, we tested whether applying the HBP substrate GlcN alone was sufficient to modulate inhibitory transmission, as this approach more closely recapitulates the endogenous regulation of cellular O-GlcNAcylation.

Experimental design and statistical analysis. Recordings were analyzed using Clampfit 10.6. For two-group comparisons, statistical significance was determined by two-tailed paired or unpaired Student's t-tests (parametric), or Wilcoxon matched-pairs signed rank test (non-parametric, paired). Multi-groups were analyzed using repeated measure one-way ANOVA with Sidak correction (parametric) or repeated measure two-way ANOVA with Sidak's test (non-parametric) (GraphPad Prism 8.1.0, La Jolla, CA). Data are displayed as mean ±SEM and p values less than 0.05 were considered statistically significant.